

Computer Model of the Building Envelope the Thermophysical Characteristics Determining Process

Vitalii Babak¹, Oleg Dekusha¹, Svitlana Kovtun¹, Leonid Shcherbak¹ and Sergiy Kobzar²

¹ General Energy Institute of National Academy of Sciences of Ukraine, 172, Antonovich str, Kyiv, 03150, Ukraine

² Institute of Engineering Thermophysics of NAS of Ukraine, 2a, Marii Kapnist str., Kyiv, 03057, Ukraine

Abstract

Thermophysical properties are a key factor in controlling heat losses and as a result in assessing the building's energy efficiency. For control heat losses one of the main thermophysical characteristics is the specific thermal resistance of the building envelope, which is defined as the resistance of individual characteristic zones of the envelope taking into account their area. Various calculation methods, physical and mathematical models, computational fluid dynamics (CFD) modeling and experimental studies are used to determine thermal resistance. This work combines all the above-mentioned approaches to control the thermophysical characteristics of the building. In the work, a computer simulation of the process of complex radiative and convective-conductive heat exchange during the control of the thermophysical characteristics of the building envelope was carried out, taking into account the locations of the sensors and the influence of their parameters on the control result. Validation of the CFD model was performed using experimental data and shown good convergence of the obtained results. In work also shown practical application of the CFD model for the analysis of the sensor's parameters influence on the thermophysical characteristics control of the building envelope.

Keywords

Computer model, CFD model, thermophysical characteristics, heat flux, control of the thermal resistance, heat flux sensors

1. Introduction

Thermophysical properties are a key factor in controlling heat losses and as a result in assessing the building's energy efficiency [1,2]. For control heat losses one of the main thermophysical characteristics is the specific thermal resistance of the building envelope, which is defined as the resistance of individual characteristic zones of the envelope taking into account their area [3,4]. Various calculation methods [3,4], physical and mathematical models [5,6], computational fluid dynamics (CFD) modeling [7,8] and experimental studies [9,10,11] are used to determine thermal resistance. Experimental studies of thermophysical characteristics of the building envelope defined by the ISO 9869 standard [9] have a number of significant drawbacks, among which the following should be highlighted: long duration of measurements (at least 72 hours) [12] if necessary, the experiment can be extended; the need to use a large number of sensors to obtain a representative result [13,14]; limitation of climate parameters for measurements [11, 15]. Significant uncertainties of the measurement results can be caused by large number of influencing factors such as geometric dimensions and orientation of the building [16], location of sensors [9,11], external climatic conditions [11,15, 16]. CFD modeling expands the range of solvable tasks, which are the basis for improving building envelope designs and developing optimal

Proceedings ITTAP'2023: 3rd International Workshop on Information Technologies: Theoretical and Applied Problems, November 22–24, 2023, Ternopil, Ukraine, Opole, Poland

EMAIL: vdoe@ukr.net (A. 1); olds@ukr.net (A. 2); sveta_kovtun@ukr.net (A. 3); prof_scherbak@ukr.net (A.4) SKobzar@nas.gov.ua (A. 5)
ORCID: 0000-0002-9066-4307 (A. 1); 0000-0003-3836-0485 (A. 2); 0000-0002-6596-3460 (A. 3); 0000-0002-1536-4806 (A. 4); 0000-0002-8615-4400 (A. 5)



© 2020 Copyright for this paper by its authors.

Use permitted under Creative Commons License Attribution 4.0 International (CC BY 4.0).

CEUR Workshop Proceedings (CEUR-WS.org)

operation modes of the ventilation and heating system [8,14]. For variation of ventilation systems operating modes CFD-models have become one of the main tools [17, 18]. But the created CFD models necessarily require validation according to experimental data [18].

This work combines all the above-mentioned approaches to control the thermophysical characteristics of the building envelope taking into account the locations of the sensors and the influence of their parameters on the control result.

2. Analysis of the object and the research problem

The aim of the research is to determine the distribution of the internal thermal field during the control of the thermophysical characteristics of the building envelope in typical structures by using the computer modeling results under the influence of external factors taking into account the locations and the influence of the sensors parameters.

Figure 1 shows a schematic illustration of the object under study, in particular the section of the building envelope, on which influence the external and internal fields, and also the heat flux sensor. The thermophysical properties of the building envelope are related to the external climatic and internal thermal fields, the heat transfer process.

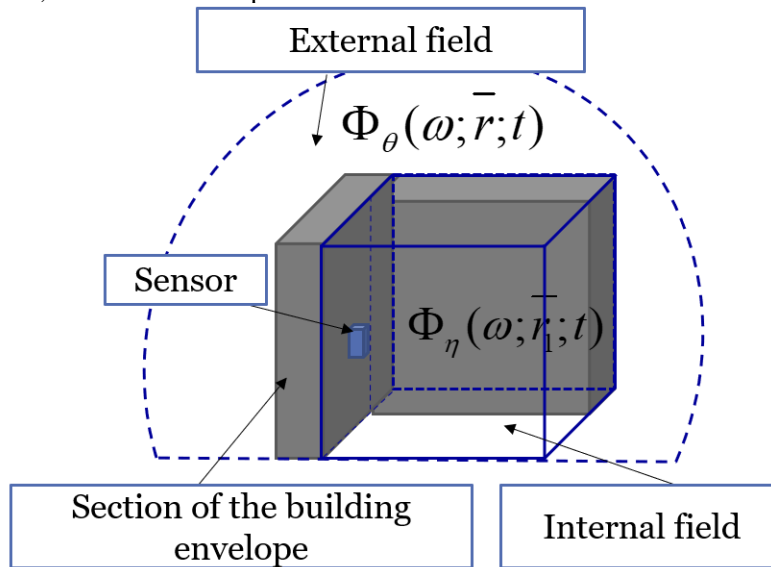


Figure 1: Schematic illustration of the relationship between the object under study, the external and internal fields, and the heat flux sensor during a computer simulation experiment

One of the main objects of a computer experiment is models of external and internal fields. The analysis of publications with the results of research on this issue [3,6,19,20] confirmed the complexity of building and substantiating mathematical models of external and internal fields of corresponding copies of the display of real meteorological fields.

Based on the analysis of the results of such publications, a mathematical model of the climatic component of the atmospheric meteorological field in the form of a parametric random field can be given in a general form

$$\{\Phi_{\theta}(\omega; \bar{r}; t), \omega \in \Omega, \bar{r} = (x, y, z) \in G \subset R^3, t \in T\} \quad (1)$$

where $\theta = \langle T, P, V, H \rangle$ - field parameters tuple, T – temperature, P- pressure, V – air speed, H – humidity.

Model (1) allows decomposition into the following corresponding additive components at the annual time interval of observation:

$$\Phi_{\theta}(\omega; \bar{r}; t) = A_{\theta}(\bar{r}, t) + B_{\theta}(\bar{r}, t) + \xi_{\theta}(\omega, \bar{r}, t) \quad (2)$$

Where deterministic part of the climatic component of the atmospheric meteorological field $A_{\theta}(\bar{r}, t)$ obtained by statistical averaging over the ensemble of implementations which is characterized by seasonal climate changes (winter, spring, summer, autumn);

The deterministic harmonic part of the climatic component $B_{\theta}(\bar{r}, t)$ obtained from the ensemble of implementations which are determined by the daily cycle (day, night).

The stochastic part of the climatic component $\xi_\theta(\omega, \bar{r}, t)$ of the atmospheric meteorological field characterizes its corresponding fluctuations.

The thermophysical characteristics and properties of the building envelope are generally described by the appropriate transformation operator Y under the action of an external field. Thus, in general, the internal (in the middle of the building envelope) random field is described by the following expression:

$$\{\Phi_\eta(\omega; \bar{r}_1; t) = Y[\Phi_\theta(\omega; \bar{r}; t)], \omega \in \Omega, \bar{r}_1 = (x_1, y_1, z_1) \in G_1 \subset G, t \in T\} \quad (3)$$

The tuple of control parameters $\eta = (\lambda; RH; \varepsilon)$ includes the coefficient of thermal conductivity (thermal resistance), relative humidity, emission coefficient, which in general are functions of the above parameters of the fields.

The following assumptions were used to obtain the results of a computer experiment with the aim of verifying the mathematical model of the internal thermal field based on the measurement data.

Using the hypothesis of a fixed state of the atmosphere during the computer experiment, the specified parameters of the climatic component were considered numerical values. For more detailed analysis, the building envelope is divided into characteristic measurement zones for analysis using computer models. One of such characteristic zones is the insulated section of the wall facade without the presence of heating devices.

3. CFD model of heat exchange in the characteristic zone of the building envelope

3.1. Description of the model

The simulation was carried out using the ANSYS CFX software. The model includes fluid and solid computational domains. The liquid domain is a layer of air. The geometry of the studied object was constructed using the ANSYS Design Manager. Since one of the modeling tasks is to assess the effect of sensors on the distribution of the thermal field on the surface of the building envelope structure during tests, heat flux sensors were introduced into the model as separate elements installed on the wall. Also, to match the calculation grid, separate zones were formed in the solid area, which coincide in size with the heat flux sensors. The general appearance of the 3D model is shown in Fig. 2.

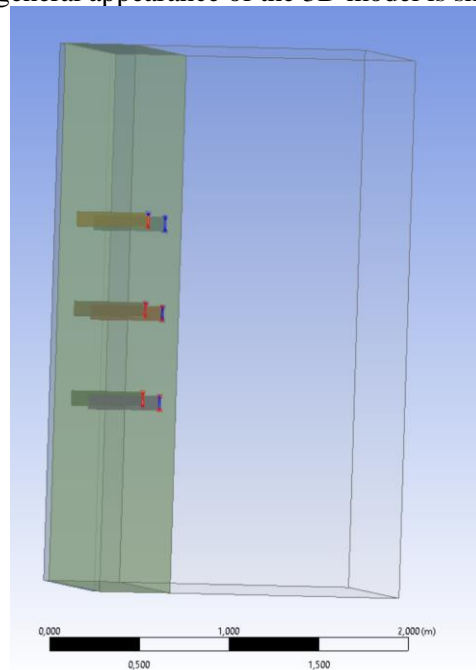


Figure 2: General view of the 3D model

For perform CFD modeling, an unstructured combined calculation grid was used, built using the ANSYS CFX Mesh generator (Fig. 3). The calculated grid consisted of 2053866 elements and 1446712 nodes. It should be noted that each heat flux sensor consisted of 43200 elements and 51667 nodes.

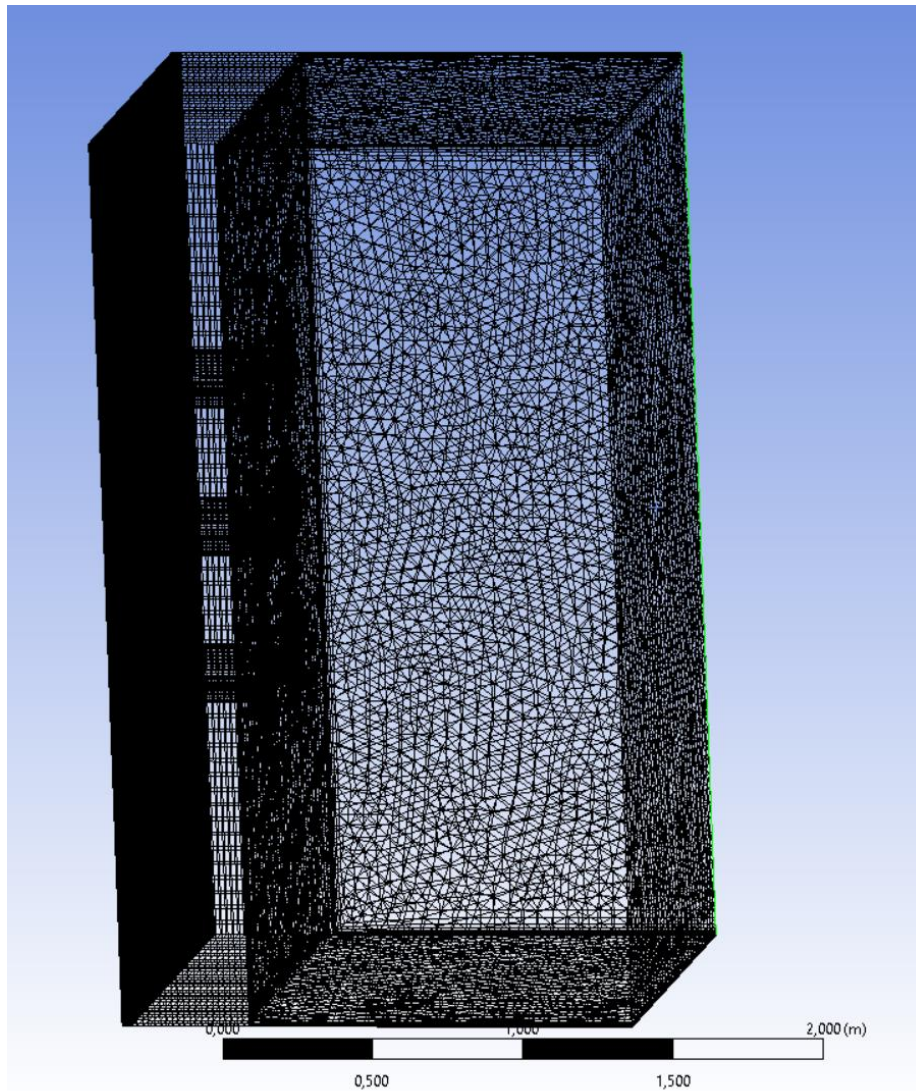


Figure 3 Computational grid of the CFD model

The solid calculation areas are layers of polyurethane foam (PUF), concrete blocks, and heat flux sensors, the characteristics of which are given in Table 1. Testing of the elements of the building's enclosing structure was carried out by the sampling method according to ISO 9869-1 [4,21]. For this purpose, a sample of polyurethane foam (PUF) taken from the investigated building was studied in a system based on the Heat Flow Meter device in accordance with ISO 8301 [22], the characteristics are shown in Table 1 [21].

Table 1.

Characteristics of the materials of enclosure construction of the building

| Material | Thickness, m | Thermal conductivity, W/(m·K) |
|-----------------|--------------|-------------------------------|
| PUF | 0.03 | 0.0346 |
| Concrete blocks | 0.40 | 0.5200 |

The characteristics of heat flux sensors are defined in the publication [23]

Complex conductive, convective and radiative heat exchange is considered in the model, which makes it possible to analyze in detail the factors influencing the results of control the thermophysical characteristics of the building envelope (Fig. 4).

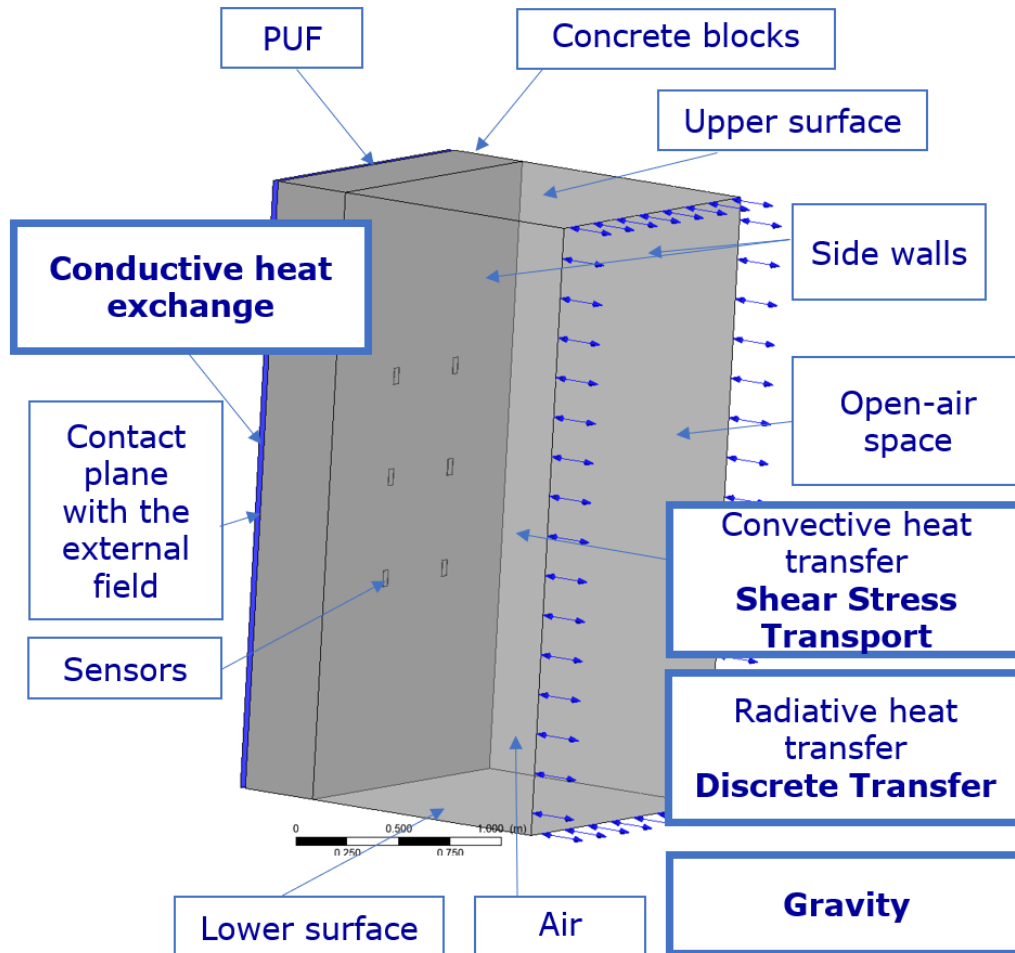


Figure 4 CFD model of the characteristic zone of the building envelope.

Conductive heat exchange between solid calculation areas is described using the heat conduction equation [7,8,25]. The influence of gravity is taken into account by setting the appropriate value [7,8].

All subdomains were connected by interface bonds to ensure the condition of heat flux constancy at the fluid–solid boundary of each subdomain.

Radiative heat transfer is described using the Discrete Transfer model implemented in ANSYS CFX, which performed best according to the results of previous studies [24]. At the same time, emission coefficients are set for each region.

To describe the convective heat transfer in the liquid calculation domain, the Shear Stress Transport turbulence model built into ANSYS CFX was used [7,8,25].

Boundary conditions are given as follows.

- The side walls are considered in the adiabaticization mode.
- The lower and upper surfaces are considered as walls with temperatures of 17.5 and 18.5 °C and heat transfer coefficients of 1.66 W/(m² K) and 2.1 W/(m² K) , respectively [25].
- The far wall was set as an open-air space with a temperature distribution of 17.5 to 18.5 °C along the height.
- The contact plane with the external field was set as temperature with distribution from height 2.71 to 2.88 °C.

3.2. Calculation results

Figures 5 and 6 show velocity fields in cross-sections of the building envelope. For the vertical position, the fields in the "XZ" plane that pass through the heat flux sensors are shown.

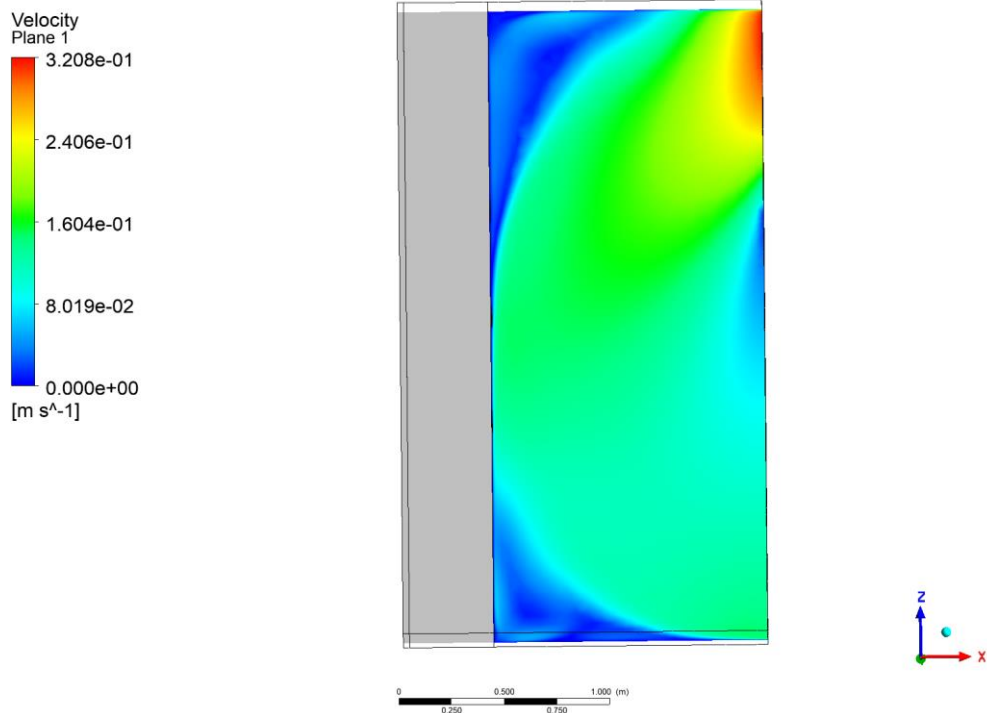


Figure 5 The velocity field in the "XZ" plane that passes through the heat flow sensors.

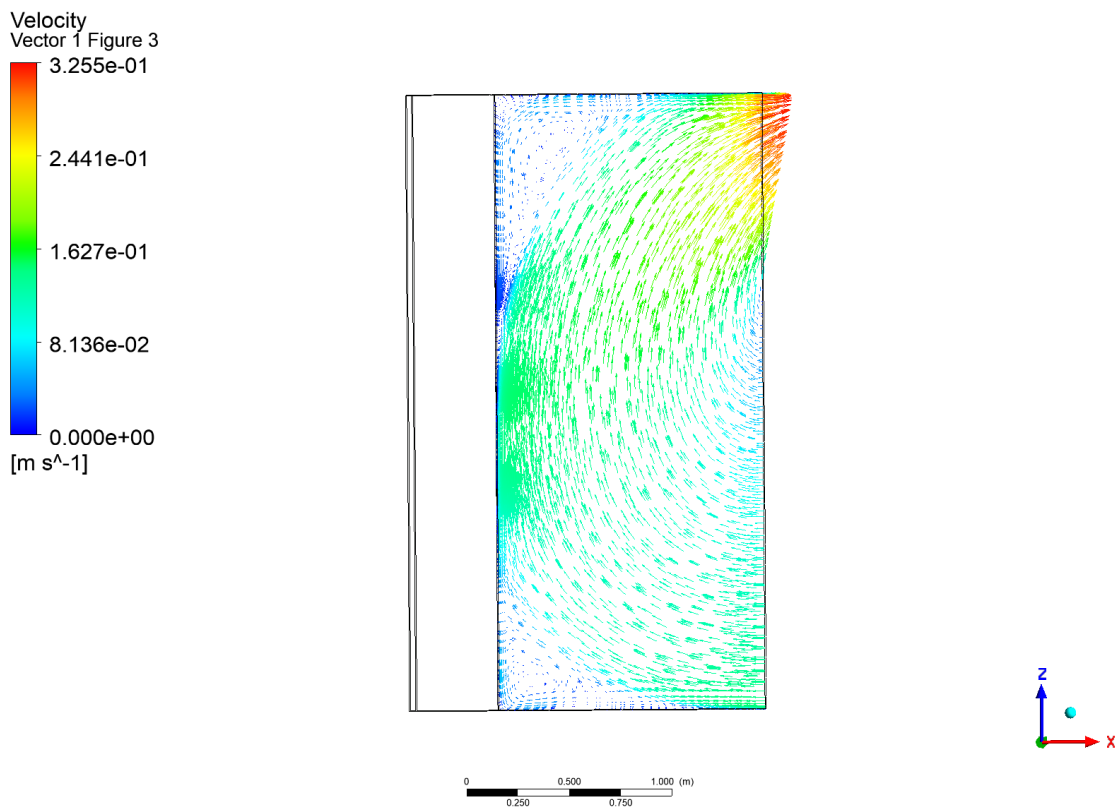


Figure 6 Velocity vector field in the "XZ" plane passing through the heat flux sensors.

As can be seen from the figures, there is an increase in speed in the upper and middle sensor zones in the wall layer, but the air speed does not exceed 0.2 m/s, which does not have a significant impact on the measurement results [7,8,25]. It should be noted that the air properties include a radiation absorption coefficient equal to 0.01.

The temperature distribution in the "XZ" plane is shown in Fig. 7.

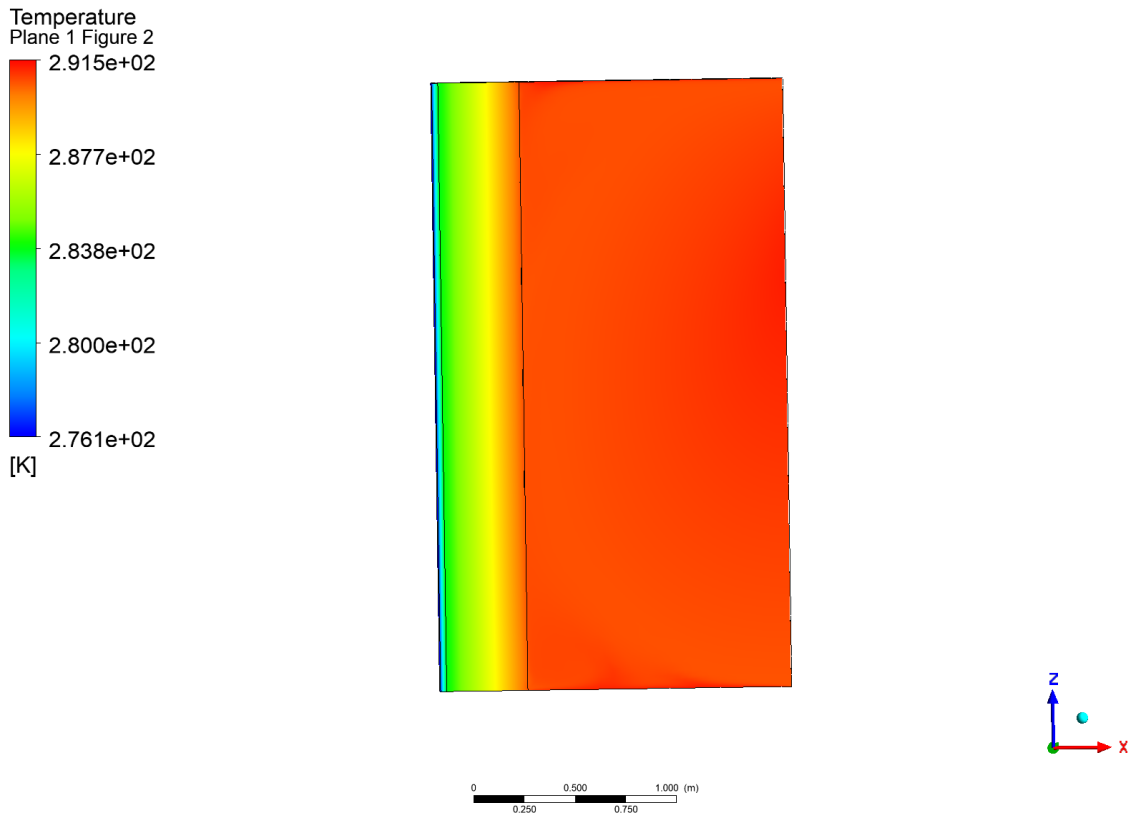


Figure 7 The temperature field in the "XZ" plane that passes through the heat flux sensors.

As noted earlier, important in the analysis is the influence of the presence of sensors on the heat flux measurement results. For this, cross-sections on the area "ZX" and "XY" were constructed, which pass through the center of the q9 sensor. The change in the temperature field of the wall surface due to the installation of the q9 sensor is shown in Fig. 8.

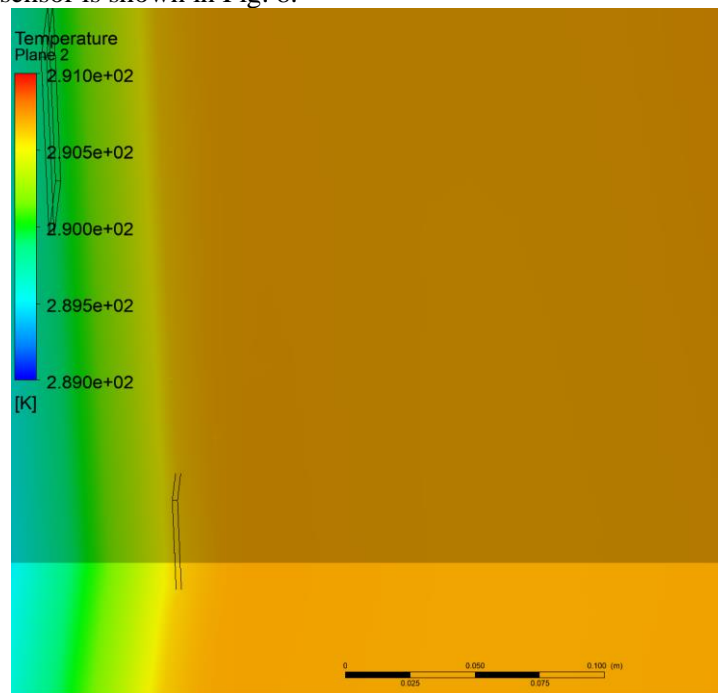


Figure 8 The temperature field in the plane "XZ" and "XY" that pass through the center of the sensor q9.

The temperature distributions on the axes of the heat flux sensor q9 and near it are shown in Fig. 9.

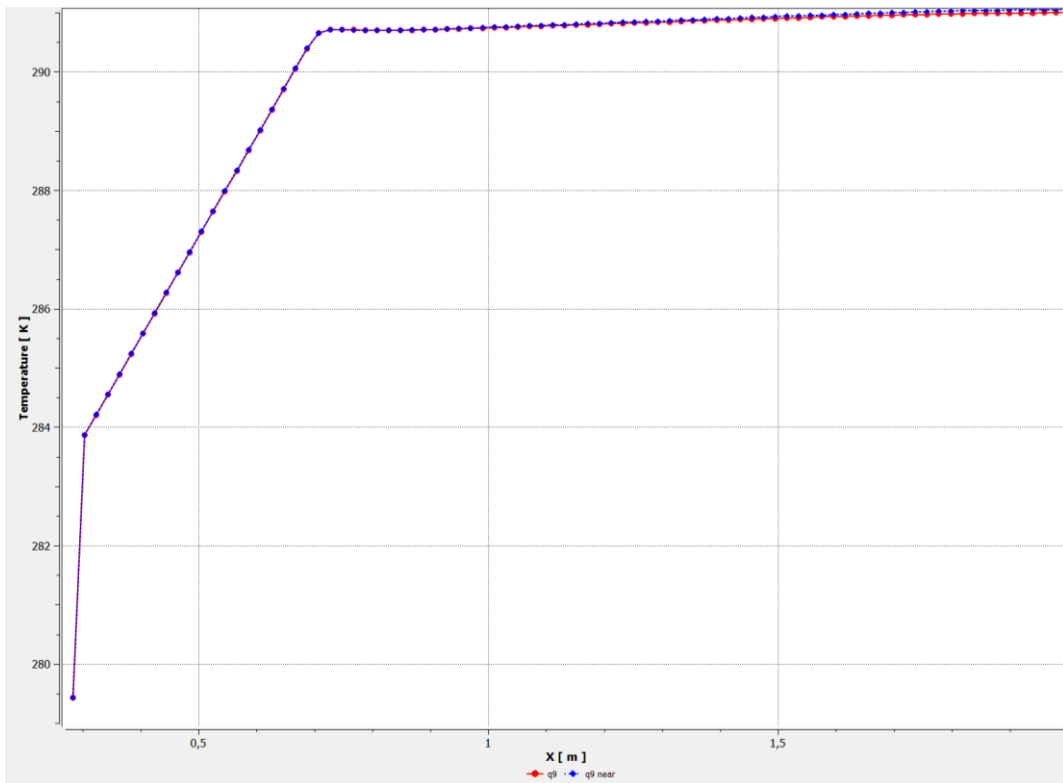


Figure 9 Temperature distribution on the axes of the heat flux sensor q9 and near it

Based on the results of calculations carried out in Ansys CFX Post, the maximum difference between the values of the temperature of the sensor and the surface of the envelope does not exceed 0.02 K.

3.3. Model validation

For the CFD model validation an experiment conducted on a characteristic zone of the wall section (Fig. 10). Heat flux was measured by bimetallic heat flux sensors (Ni-Const). Type L thermocouples were used to measure temperature. Calibration of heat flux sensors was carried out by the radiation method [23]. L-type thermocouples with individual calibration were used as sensors for measuring the external temperature [26].

An information and measurement system with the following characteristics was used to register the signals of temperature and heat flux sensors [26]:

- 8-channel ADC with 16-bit bit rate and 10 Hz conversion frequency;
- adjustment and calibration of the dynamic range;
- support for the RS-485 industrial interface and addressing, which makes it possible to create a measuring network.

The time of one measurement cycle was set to 30 s.

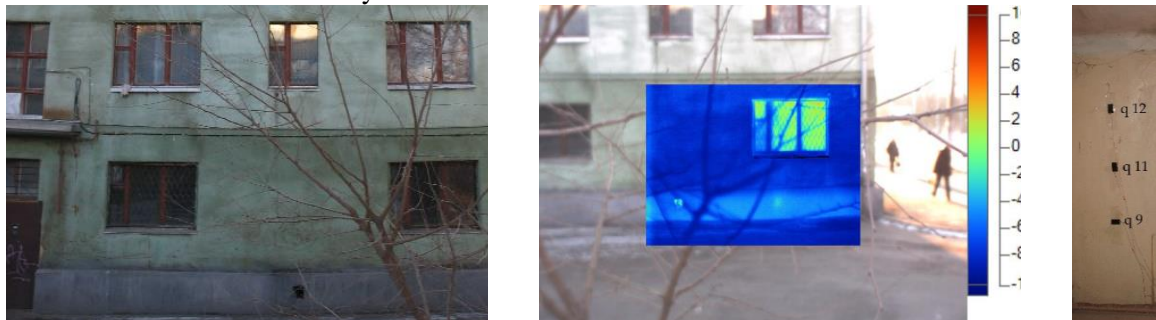


Figure 10 External appearance and thermogram of the building envelope and sensor installation locations on the inner surface of the building wall

In addition to experimental measurements, testing of elements of the building envelope was carried out by the method of sampling in accordance with ISO 9869-1 [4,24].

Before installing the heat flux sensors, a qualitative analysis of the building was carried out using the method given in ISO 6781 [27] and Information and measurement technology [28]. Thermal images of the exterior of the building where the sensors were placed are shown in Figure 10.

For verification, the values of temperature and heat flux measured by sensors in characteristic zones during the experiment [24] were chosen. The results are shown in Table 2

Table 2

Comparison of the results of experimental studies and CFD modeling

| | q9, W/m ² | Tsi9, °C | Tse9, °C | q11, W/m ² | Tsi11, °C | Tse11, °C | q12, W/m ² | Tsi12, °C | Tse12, °C |
|------------|-------------------------|-------------|-------------|--------------------------|--------------|--------------|--------------------------|--------------|--------------|
| Experiment | 9.02 | 17.4 | 2.87 | 9.87 | 17.57 | 17.57 | 9.85 | 17.79 | 2.88 |
| CFD | 8.77 | 17.44 | 2.71 | 9.5 | 17.48 | 17.48 | 9.66 | 17.49 | 2.88 |

From the analysis of the Table 2 it was found that the deviation between the results of CFD modeling and experimental data did not exceed 0.3 K for the temperature and 0.3 W/m² for the heat flux, which indicates a good convergence of the obtained results and the adequacy of the created CFD model.

4. CFD model practical application

One of the advantages of proposed CFD model lays in the inclusion of the heat flux sensors with corresponding physical parameters. Which gives possibility for the analysis of the sensor's parameters influence on the thermophysical characteristics control of the building envelope.

For this task, the emission coefficient of the q9 sensor was changed to 0.71, which corresponds to the value of the TES1-12703 sensor described in the article [24], while all other parameters of the model remain unchanged.

Figure 11 shows the temperature distribution on the axes of the heat flux sensor and along it.

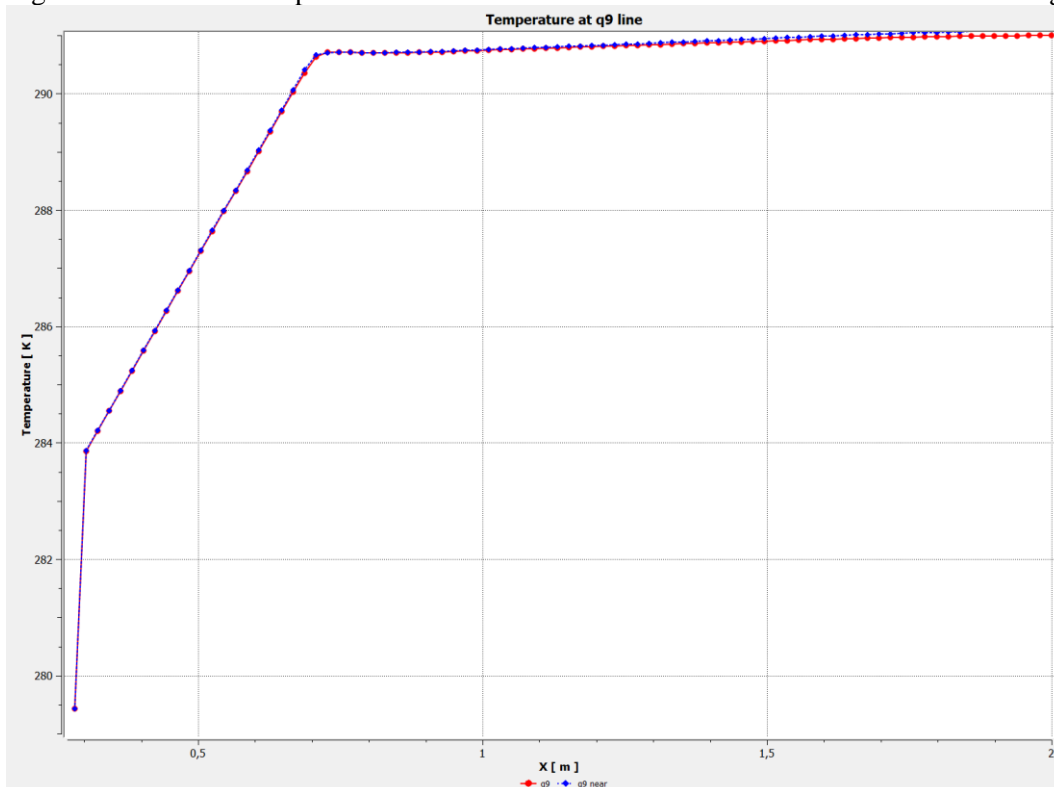


Figure 11 Temperature distribution on the axes of the heat flux sensor q9 with an emission of 0.71

Table 3 shows the results of calculations of the heat flux in the area of the sensor q9, carried out in Ansys CFX Post.

Table 3.

Heat fluxes in sensor q9 zone

| Experiment q9, W/m ² | CFD q9 ε=0.88, W/m ² | CFD q9 ε=0.71, W/m ² |
|---------------------------------|---------------------------------|---------------------------------|
| 9.02 | 8.77 | 7.6 |

From the data presented in Table 3, it follows that the change in the emission factor led to a difference in the results of simulation and experiment by more than 2 W/m². An assessment of the effect on the direct result of determining the thermal resistance of the enclosing structure was carried out. For this, the results in all four cases were compared. The value of the thermal resistance is calculated according to the following expression (4):

$$R_{HFM} = \frac{T_{si} - T_{se}}{q} \quad (4)$$

The comparison of the obtained results was carried out by calculating the relative deviation according to the following expression (5):

$$DEV = \left| \frac{R_{HFM} - R_C}{R_C} \right| \cdot 100 \%, \quad (5)$$

where R_C is the theoretical value calculated according to the ISO 9869 [4].

The results of the comparison are shown in Table 4

Table 4

Comparison of the results of experimental studies and modeling

| | R_C | R_{9HFM} | $R_{9CFD}, \epsilon=0.88$ | $R_{9CFD}, \epsilon=0.71$ |
|-----------------------------|-------|------------|---------------------------|---------------------------|
| Value, (m ² K)/W | 1.64 | 1.66 | 1.67 | 1.95 |
| Deviation, % | | 1.40 | 0.57 | 17.51 |

Based on the results of the comparison, the deviation for this case is 17.51%.

5. Conclusions

In the work, a computer simulation of the process of complex radiative and convective-conductive heat exchange during the control of the thermophysical characteristics of the building envelope was carried out, taking into account the locations of the sensors and the influence of their parameters on the control result. A general description of the heat exchange process of the building envelope using a mathematical model of an external random field, its transformation operator, which is characterized by the thermophysical properties of the building envelope and the resulting internal random field, is given.

As a result of computer CFD modeling, the distribution of the temperature and the air velocity field of the internal thermal field was obtained, which made it possible to establish the absence of increased turbulence in the area where the heat flux sensors are located. According to the results of validation of the created CFD model using experimental data, it was found that the deviation does not exceed 0.3 K for temperature and 0.3 W/m² for heat flux.

The work also shows the case when the emission coefficient of the sensor is reduced by 0.16 units, the difference in the values of the heat flux through the zone of its installation is more than 2 W/m². At the same time, the deviation of the result of control the thermal resistance of the building envelope is 17.51%.

Therefore, the use of the created CFD model is promising from the point of view of the analysis of the process of controlling the thermophysical characteristics of the building envelope, taking into account the influence of both external factors and the applied tools for in-situ tests.

6. Acknowledgements

These researches have been performed within of the scientific program «Information technology for energy audit of buildings as a component of the energy security of the country».

7. References

- [1] Gong, M.; Wang, J.; Bai, Y.; Li, B.; Zhang, L. Heat load prediction of residential buildings based on discrete wavelet transform and tree-based ensemble learning. *Journal of Building Engineering*. 2020, 32, 101455. <https://doi.org/10.1016/j.jobee.2020.101455>.
- [2] Final Energy Consumption by Sector. Report of the European Parliamentary Research Service. Available online: <https://epthinktank.eu/2022/06/16/monitoring-the-energy-situation-in-the-eu-june-2022/final-energy-consumption-by-sector/>.
- [3] UNI/TS 11300-1: 2014 – Energy Performance of Buildings – Part 1: Determination of the Building Thermal Energy Demand for Climatization in Winter and Summer Season
- [4] ISO 9869-1. Thermal Insulation – Building Elements – In-Situ Measurement of Thermal Resistance and Thermal Transmittance – Part 1: Heat Flow Meter Method; ISO: Geneva, Switzerland, 2014.
- [5] E. Sassine, Y. Cherif, E. Antczak, Parametric identification of thermophysical properties in masonry walls of buildings, *J. Build. Eng.* 25, 2019
- [6] De Wilde, P. The gap between predicted and measured energy performance of buildings: A framework for investigation. *Autom. Constr.*, 41, 40–49. 2014
- [7] Peter V. Nielsen Fifty years of CFD for room air distribution *Building and Environment* Volume 91, Pages 78-90 doi:10.1016/j.buildenv.2015.02.035
- [8] B. Yang, A.K. Melikov, A. Kabanshi, C. Zhang, F.S. Bauman, G. Cao, H. Awbi, H. Wigö, J. Niu, K.W.D. Cheong, K.W. Tham, M. Sandberg, P.V. Nielsen, R. Kosonen, R. Yao, S. Kato, S.C. Sekhar, S. Schiavon, T. Karimipannah, X. Li, Z. Lin, A review of advanced air distribution methods - theory, practice, limitations and solutions, *Energy and Buildings*, Volume 202, 2019, 109359, ISSN 0378-7788, doi:10.1016/j.enbuild.2019.109359.
- [9] ISO 9869-1, Thermal insulation–Building elements–In-situ measurement of thermal resistance and thermal transmittance–Part 1: Heat flow meter method, International Organization for Standardization, ISO, Geneva, Switzerland, 2014.
- [10] Meng, X.; Yan, B.; Gao, Y.; Wang, J.; Zhang, W.; Long, E. Factors affecting the in situ measurement accuracy of the wall heat transfer coefficient using the heat flow meter method. *Energy Build.* 2015, 86, pp. 754–765. doi:10.1016/j.enbuild.2014.11.005
- [11] Evangelisti, L.; Guattari, C.; Asdrubali, F. Comparison between heat-flow meter and Air-Surface Temperature Ratio techniques for assembled panels thermal characterization. *Energy and Buildings*. 2019, Vol. 203, 109441. doi:10.1016/j.enbuild.2019.109441
- [12] Gaspar, K.; Casals, M.; Gangoles, M. Review of criteria for determining HFM minimum test duration. *Energy Build.* 2018, 176, 360–370. <https://doi.org/10.1016/j.enbuild.2018.07.049>.
- [13] Cucumo, M.; Ferraro, V.; Kaliakatsos, D.; Mele, M. On the distortion of thermal flux and of surface temperature induced by heat flux sensors positioned on the inner surface of buildings. *Energy Build.* 2018, 158, pp. 677–683. doi:10.1016/j.enbuild.2017.10.034
- [14] Evangelisti L, Guattari C, Asdrubali F. Influence of heating systems on thermal transmittance evaluations: simulations, experimental measurements and data postprocessing. *Energy Build.* 2018; 168: 180–90. <https://doi.org/10.1016/j.enbuild.2018.03.032>
- [15] Gori, V.; Elwell, C.A. Estimation of thermophysical properties from in-situ measurements in all seasons: quantifying and reducing errors using dynamic grey-box methods. *Energy Build.* 2018, 167, 290–300 <https://doi.org/10.1016/j.enbuild.2018.02.048>.
- [16] Soares, N.; Martins, C.; Goncalves, M.; Santos, P.; da Silva, L.S.; Costa, J.J. Laboratory and in-situ non-destructive methods to evaluate the thermal transmittance and behavior of walls, windows, and construction elements with innovative materials: a review. *Energy Build.* 2019, 182, 88–110. <https://doi.org/10.1016/j.enbuild.2018.10.021>
- [17] M. Hurnik, M. Blaszcok, Z. Popiolek, Air distribution measurement in a room with a sidewall jet: A 3D benchmark test for CFD validation, *Building and Environment*, Volume 93, Part 2, 2015, doi:10.1016/j.buildenv.2015.07.004.
- [18] Yang Wang, Fu-Yun Zhao, Jens Kuckelkorn, Di Liu, Jun Liu, Jun-Liang Zhang, Classroom energy efficiency and air environment with displacement natural ventilation in a passive public school building, *Energy and Buildings*, Volume 70, 2014, pp. 258-270, doi:10.1016/j.enbuild.2013.11.071.

- [19] Zaporozhets, A., Khaidurov, V. Mathematical Models of Inverse Problems for Finding the Main Characteristics of Air Pollution Sources. *Water, Air, & Soil Pollution*, 2020, 231(12), 563. <https://doi.org/10.1007/s11270-020-04933-z>
- [20] Wang, H.; Zhu, T.; Zhu, X.; Yang, K.; Ge, Q.; Wang, M.; Yang, Q. Inverse estimation of hot-wall heat flux using nonlinear artificial neural networks. *Measurement*. 2021, 181, 109648. <https://doi.org/10.1016/j.measurement.2021.109648>.
- [21] Hotra O., Kovtun S., Dekusha O., Grądz Ż., Babak V., Styczeń J. Analysis of Low-Density Heat Flux Data by the Wavelet Method, *Energies*, 16 (1), art. no. 430, 2023, DOI: 10.3390/en16010430
- [22] ISO 8301. Thermal Insulation – Determination of Steady-State Thermal Resistance and Related Properties – Heat Flow Meter Apparatus; ISO, Geneva, Switzerland, 1991.
- [23] Hotra, O.; Kovtun, S.; Dekusha, O. Analysis of the characteristics of bimetallic and semiconductor heat flux sensors for in-situ measurements of envelope element thermal resistance. *Measurement*. 2021, 182, 109713. <https://doi.org/10.1016/j.measurement.2021.109713>
- [24] Dekusha, O., Babak, V., Vorobiov, L., Dekusha, L., Kobzar, S. & Ivanov, S. The heat exchange simulation in the device for measuring the emissivity of coatings and material surfaces. *IEEE 39th International Conference on Electronics and Nanotechnology “ELNANO-2019”*. pp. 301-304, 2019. Retrieved from: DOI: 10.1109/ELNANO.2019.8783537
- [25] Di Pasquale, Davide Rona, Aldo Garrett, S. A selective review of CFD transition models. 39th AIAA Fluid Dynamics Conference. 2009
- [26] Babak, V.; Dekusha, O.; Kovtun, S.; Ivanov, S. Information-measuring system for monitoring thermal resistance. *CEUR Workshop Proceedings*. 2019, 2387, 102-110. Available online: <http://ceur-ws.org/Vol-2387/20190102.pdf> (accessed on 25 November 2022).
- [27] ISO 6781-2015. Thermal performance of building – Qualitative detection of thermal irregularities in building envelopes – Infrared method
- [28] Dekusha O.L., Kovtun S.I., Romanenko V.V., Sozonov S.V. Information-measuring Technology for Buildings Enclosing Structures Thermal Resistance Control *CEUR Workshop Proceedings*, 3309, 2022, pp. 301 – 313